


Conductive and superhydrophobic cotton fabric through pentaerythritol tetrakis(3-(3,5-di-*tert*-butyl-4-hydroxyphenyl)propionate) assisted thermal reduction of graphene oxide and modification with methyltrichlorosilane

T. Makowski  · M. Svyntkivska · E. Piorkowska · U. Mizerska · W. Fortuniak · D. Kowalczyk · S. Brzezinski

Received: 28 March 2018 / Accepted: 3 July 2018 / Published online: 11 July 2018
© Springer Nature B.V. 2018

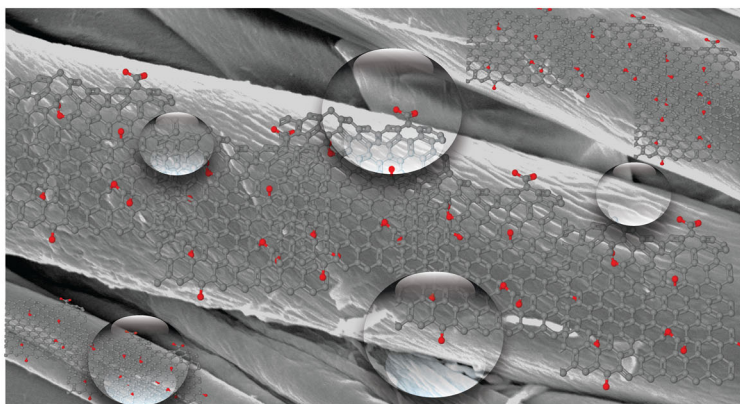
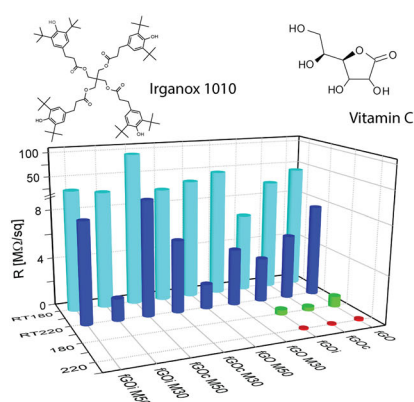
Abstract Pentaerythritol tetrakis(3-(3,5-di-*tert*-butyl-4-hydroxyphenyl)propionate), an antioxidant widely applied in the plastic industry, was used to assist thermal reduction of graphene oxide (GO) on a cotton fabric in air. L-ascorbic acid was also applied for comparison. GO was deposited on the fabric by the padding method. Reduction of GO deposited on fiber surfaces at 180 and 220 °C in air imparted electrical conductivity. For all the materials the conductivity worsened after the reduction during cooling and during the first hours of storage at room conditions.

However, the most stable effect of GO reduction was achieved using pentaerythritol tetrakis(3-(3,5-di-*tert*-butyl-4-hydroxyphenyl)propionate), which assisted the reduction of GO at both 180 and 220 °C, and allowed to obtain the cotton fabric with a stable surface resistivity of 6.6 and 3.7 MΩ/sq, respectively. Moreover, superhydrophobicity of the conductive fabric was achieved by modification with methyltrichlorosilane in an anhydrous environment.

T. Makowski (✉) · M. Svyntkivska ·
E. Piorkowska · U. Mizerska · W. Fortuniak
Centre of Molecular and Macromolecular Studies Polish
Academy of Sciences, Sienkiewicza 112, 90-363 Lodz,
Poland
e-mail: tomekmak@cbmm.lodz.pl

D. Kowalczyk · S. Brzezinski
Textile Research Institute, Brzezinska 5/15, 92-103 Lodz,
Poland

Graphical abstract



Keywords Cotton · Graphene oxide · Reduction · Kelvin probe force microscopy · Lotus effect

Introduction

In recent years, conductive composites based on environment-friendly substrates, including those based on cotton fabrics, have attracted great interest. Being lightweight and flexible, such conductive textiles have a wide range of uses in various industries, for example as flexible energy storages (Jost et al. 2011), conductive and flame retardant fabrics (Attia et al. 2015), sensors for human gesture recognition (Huang et al. 2017), flexible strain sensors (Ren et al. 2017), electromagnetic radiation shields (Nooralian et al. 2016), components of supercapacitors (Huang et al. 2016; Xu et al. 2015) and solar cells (Sahito et al. 2015, 2016). Applications of graphene for modification of textiles are rare due to difficulties in its use in the form of aqueous dispersions. Owing to its structure and the presence of functional groups (hydroxyl, carboxyl, carbonyl and epoxy) graphene oxide (GO) can be dispersed in liquids and deposited on textiles. Van der Waals forces and hydrogen bonds between exfoliated GO and cellulose fibers assure strong adhesion and enable efficient coating, even by means of dip coating (Shateri-Khalilabad and Yazdanshenas 2013b; Zhang et al. 2016). GO coated fabrics can be further modified chemically and/or physically, resulting in smart textiles (e-textiles); especially the reduction of GO on surfaces of cotton fibers can lead to

conductive materials. It is worth noting that only low cytotoxic effect of GO at the skin level after long exposure was reported (Bussy et al. 2015; Pelin et al. 2017). However, many applications of electrically conductive fabrics do not require direct contact with skin.

Thermal reduction of GO requires high temperature (Huh 2011). However, chemical reduction of GO is also possible by numerous reducing agents (Chua and Pumera 2014), although in many cases the mechanisms of the reduction are not understood. One of them is L-ascorbic acid (Vitamin C), environmentally friendly and able to substitute hydrazine (Fernandez-Merino et al. 2010; Zhang et al. 2010a), although exhibiting low stability at elevated temperature (Juhász et al. 2012).

The electrical conductivity of GO modified textiles depends on a number of deposited layers, reducing agent applied and conditions of the reduction process (time and temperature, reducing agent concentration) (Shateri-Khalilabad and Yazdanshenas 2013a). However, it is rather obvious that during reduction of GO on textiles, the textiles cannot be exposed to too high temperature or harmful reducing agents. On the other hand, chemical reduction of GO at relatively low temperature often requires a long time, for instance, GO modified cotton samples had to be immersed in aqueous solution of an ascorbic acid at 95 °C for 1 h (Shateri-Khalilabad and Yazdanshenas 2013a). Although thermal reduction of GO is usually carried out in the oxygen-free atmosphere (Pei and Cheng 2012), the reduction of GO on fabrics in such conditions has limited applicability. It was recently

demonstrated (Tegou et al. 2016) that thermal treatment of GO films in air at relatively low temperature, up to 300 °C, for 1 h, can enhance electrical conductivity.

The important property of modified cotton fabric is its hydrophobicity/philicity. The surface is hydrophobic if the water contact angle (WCA) exceeds 90°, and is superhydrophobic if WCA exceeds 150°. However, it is clear now that a single parameter cannot characterize wetting of rough surfaces, for instance on hydrophobic surfaces the rose petal effect and the lotus effect are observed.

It is worth noting that GO modified cotton textiles after reduction of GO to reduced GO (rGO) can exhibit an adhesive type of hydrophobicity similar to that present in rose petals (Tissera et al. 2015). However, imparting superhydrophobicity to cotton fabrics coated with carbon nanoparticles by modification with methyltrichlorosilane (MTCS) was also reported (Makowski et al. 2014; Shateri-Khalilabad and Yazdanshenas 2013b). The modification resulted in the formation of micro and nanostructures causing the lotus effect. After modification with MTCS, the cotton fabric showed superhydrophobicity whereas conductivity was preserved (Shateri-Khalilabad and Yazdanshenas 2013b). In addition, the hydrophobic properties of MTCS modified cotton fabric depended on humidity at which the fabric was conditioned (Makowski et al. 2014).

It is also worth noting that in the plastic industry antioxidants are applied to prevent oxidative degradation of polymers during processing and further use. One of them is pentaerythritol tetrakis(3-(3,5-di-*tert*-butyl-4-hydroxyphenyl)propionate) known under trade names as, for example, Irganox 1010 or Anox 20. It is harmless for humans, approved in many countries for food contact applications and often used in food packaging polymers (Marcato et al. 2003; Onghena et al. 2015; Rani et al. 2017). The aim of this work was to demonstrate the ability of pentaerythritol tetrakis(3-(3,5-di-*tert*-butyl-4-hydroxyphenyl)propionate) to assist thermal reduction of GO deposited on a cotton fabric. Unlike in the previous studies, the thermal reduction of GO on the fabric was carried out in air and for short time only. The fabric specimens were heated to 180 or 220 °C and annealed at these target temperatures for short times, which was sufficient to impart electric conductivity to the modified fabric. For comparison, L-ascorbic acid used

successfully to reduce GO by others (Fernandez-Merino et al. 2010), was also applied to assist the thermal reduction of GO.

Then, superhydrophobicity of the fabrics was achieved with MTCS treatment.

Experimental

Materials

Reagents and solvents

L-ascorbic acid—vitamin C (C₆H₈O₆), with purity of 98%, and Irganox 1010, that is pentaerythritol tetrakis(3-(3,5-di-*tert*-butyl-4-hydroxyphenyl)propionate) (C₇₃H₁₀₈O₁₂), were provided by POCH (Poland) and BASF (Germany), respectively. Chemical structures of both vitamin C and Irganox 1010 are shown in Scheme 1. Methyltrichlorosilane (CH₃Cl₃, Si) (MTCS) with purity of 97% was purchased from Sigma-Aldrich Poland. Acetone with purity of 99% and toluene with purity of 99.5% were supplied by POCH and CHEMPUR (Poland), respectively.

Graphene oxide (GO)

0.6 wt% aqueous dispersion of GO was purchased from Graphene Laboratories, Inc. (USA); single layer > 80%, flake size of 0.5–5 μm. For a further use, the dispersion was diluted with water to decrease the concentration of GO to 0.1 wt%.

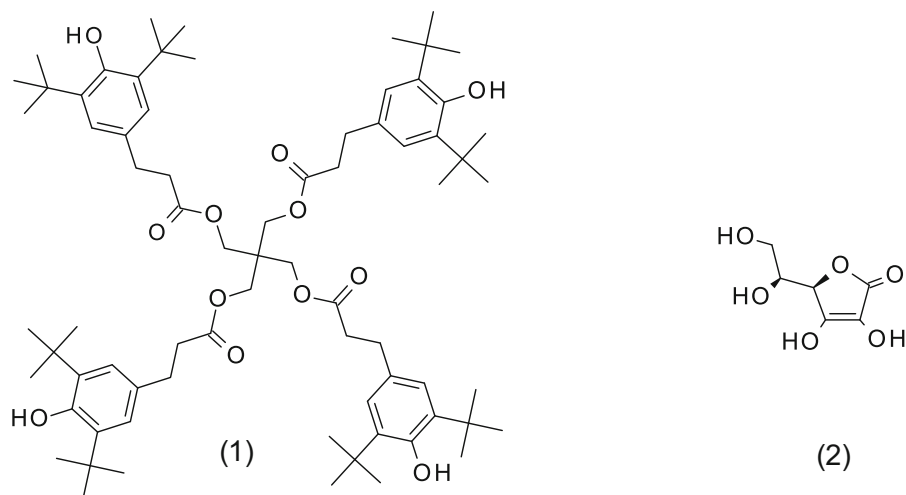
Woven fabric

The study utilized white plain weave cotton fabric 0.36 mm thick, with a surface weight of 145 ± 7 g/m², and with 295 threads/10 cm and 205 threads/10 cm in the warp and weft directions, respectively. To purify the fabric prior to a further modification, it was cleaned by diethyl ether and anhydrous ethanol extraction (Makowski et al. 2014).

Deposition of GO on fabric

Prior to use, the aqueous dispersion of GO was homogenized using an ultrasonic homogenizer Hielscher UP 200S (Hielscher, Germany, power 200 W, amplitude 30%, frequency 24 kHz) at room

Scheme 1 Chemical structure of pentaerythritol tetrakis(3-(3,5-di-*tert*-butyl-4-hydroxyphenyl)propionate) (1) and L-ascorbic acid (2)



temperature (RT) for 20–30 min. The dispersion was then deposited on the dry fabric by the padding method using a laboratory double-roll padding machine with horizontally set squeezing rollers (BENZ, Switzerland). The padding rate was 1 m/min with a squeezing rollers pressure of 15 kG/cm along the roller contact line. Then, the fabric was dried at 100 °C for 15 min. The padding and drying cycle was repeated four times.

Reduction of GO

To verify the ability of Irganox 1010 to assist the reduction of GO, and to compare its activity with that of vitamin C, reduction of GO in aqueous dispersions with both compounds was carried out. Vitamin C was dissolved in the dispersion of GO, to obtain its concentration of 0.1 wt%. To obtain an aqueous dispersion of GO with 0.1 wt% of Irganox 1010, an appropriate amount of acetone solution of the latter was added to the dispersion. The dispersions were then homogenized for 30 min using ultrasonic homogenizer Sonopuls HD 2200 (Bandelin, Germany) with a sonotrode (power 200 W, frequency 20 kHz, amplitude 40%). Then the dispersions were heated to 90 °C and held at this temperature for 30 min. The droplet of each dispersion was placed on a glass support sputtered with 70 nm thick gold layer. The gold layer ensured electrical conductivity of the support necessary for Kelvin probe force microscopy (KPFM). After evaporation of solvents, GO reduced with the assistance of vitamin C (rGO_C) or Irganox 1010 (rGO_I),

was analyzed with atomic force microscopy (AFM) and KPFM, as described below.

To reduce GO, the GO coated fabric samples positioned on glass supports were heated in Mettler Toledo Hot Stage FP82 equipped with FP90 temperature controller that enables precise control of heating or cooling rate, as well as steady temperature with a precision of 0.1 °C. The samples were heated at 10 °C/min to either 180 or 220 °C, held at these target temperatures for 15 or 1 min, respectively, and cooled to 30 °C at 10 °C/min. To study the effect of Irganox 1010, the GO coated fabric samples were dipped in 0.1 wt% acetone solution of Irganox 1010 prior to heating. For comparison, the fabric samples were dipped also in 0.1 wt% aqueous solution of vitamin C. After dipping the samples were dried at RT. In each case, the dipping and drying cycles were repeated four times. The samples are referred through this paper as fGO_C, fGO_I and fGO, where the letters C and I denote the fabrics treated with vitamin C and Irganox 1010, respectively, whereas the lack of a subscript indicates the untreated sample.

MTCS treatment

The fabric samples, after reduction of GO, were stored at room conditions for 24 h and then conditioned for 1 h at a relative humidity (RH) of 30 or 50%. Then the samples were modified by immersing in 0.5 M solution of MTCS in anhydrous toluene for 1 h at 25 °C. The modification procedure is described in detail elsewhere (Makowski et al. 2014). It must be

mentioned that MTCS treatment without prior conditioning led to nonuniform modification of surfaces. The samples modified with MTCS are denoted as, for instance, rGO₁ M50, where the number stands for RH during conditioning.

Characterization

The cotton fabrics were analyzed by reflected light microscopy with a light microscope Delta Optical (Poland) equipped with a digital camera.

The surfaces and compositions of the fabric samples were analyzed with a scanning electron microscope (SEM), JEOL 6010LA (JEOL, Japan). Prior to the examination, the sample surfaces were vacuum sputtered with 10 nm gold layer (Quorum EMS150R ES, UK).

WCA was measured with a 100-00-230 NRL goniometer (Rame-Hart, NJ) coupled with a camera and an optical system. WCA values were determined using Drop Analysis program (Stalder et al. 2006, 2010). Water sliding angles (WSA) were measured with the use of an apparatus of our own construction described in detail elsewhere (Makowski et al. 2014). To measure WCA and WSA, distilled water droplets of 5 and 10 μ l, respectively, were placed on the studied surfaces at 25 °C. Both WCA and WSA measurements were repeated five times for each material and average values were calculated (Kiuru and Alakoski 2004; Makowski et al. 2014).

Surface resistivity (R) of the cotton woven fabrics with deposited and reduced GO was measured by the two-wire method with copper electrodes positioned 1 cm apart, using Sanwa PC 7000 multimeter with acquisition software PCLink7 1.2 SANWA 2010 (Sanwa, Japan) or, in the case of R above 50 M Ω /sq, a current-source Keithley 2400C SourceMeter (USA). In each case, the results were averaged on three independent measurements.

AFM images were recorded under ambient atmosphere using Nanosurf Flex Axiom with C3000 controller (Nanosurf AG, Switzerland). The analysis of surface potential was carried out using KPFM and commercially available probes (EFM NanoWorld AG, Switzerland) with a nominal radius of curvature < 25 nm, spring constant of 2.8 N/m, a resonance frequency of 75 kHz. 512 \times 512 data points images were recorded and analyzed with SPIP software (Image Metrology, Denmark).

Uniaxial tensile drawing of fabric specimens in the form of 5 mm wide strips was performed with Linkam TST 350 Minitester (Linkam, UK) with the distance between grips of 20 mm, at the rate of 20 mm/min, at RT. Five specimens of each material were drawn in the weft direction.

Results and discussion

After holding at 90 °C for 30 min the GO suspensions blackened, indicating the occurrence of GO reduction. Longer time of the reduction resulted in sedimentation of particles. Figure 1 shows AFM and KPFM images of thus formed rGO_C and rGO₁ on a gold sputtered substrate. On the height and phase images, rGO_C platelets are discernible, whereas rGO₁ platelets do not show up. On the contrary, a surface potential contrast is clearly seen in KPFM images of both rGO_C and rGO₁ in Fig. 1c, f, respectively. The presence of rGO platelets deposited on the substrate increased the electrical resistance and resulted in a local darkening of the KPFM images. It must be mentioned that KPFM image can be recorded only for electrically conducting substances. The absence of clear height and phase images of rGO₁ platelets, despite their detection by KPFM, evidenced their very small thickness. On the other hand the KPFM image in Fig. 1f reflected the presence of flat objects with well-defined and rather straight edges, evidencing that lateral dimensions of rGO₁ platelets exceeded markedly those of rGO_C, seen in Fig. 1a–c. It is well known that vitamin C can release two protons and that the protons exhibit high binding affinity to hydroxyl and epoxide groups forming water molecules (Zhang et al. 2010b). Irganox 1010 belongs to the group of so called primary antioxidants that act as proton donors, similarly to vitamin C. The protons can be released from hydroxyl groups of Irganox 1010 and react with hydroxyl and epoxide groups of GO, similarly as in the case of vitamin C.

Figure 2 shows micrographs of the cotton fabric samples. The darkening of the fabric after thermal reduction of GO is clearly evidenced. It is worth mentioning that decomposition of cotton occurs above 240–250 °C (Poletto et al. 2013).

The results of R measurements of the cotton fabric samples during heating and annealing at 180 and 220 °C are shown in Fig. 3, evidencing the reduction

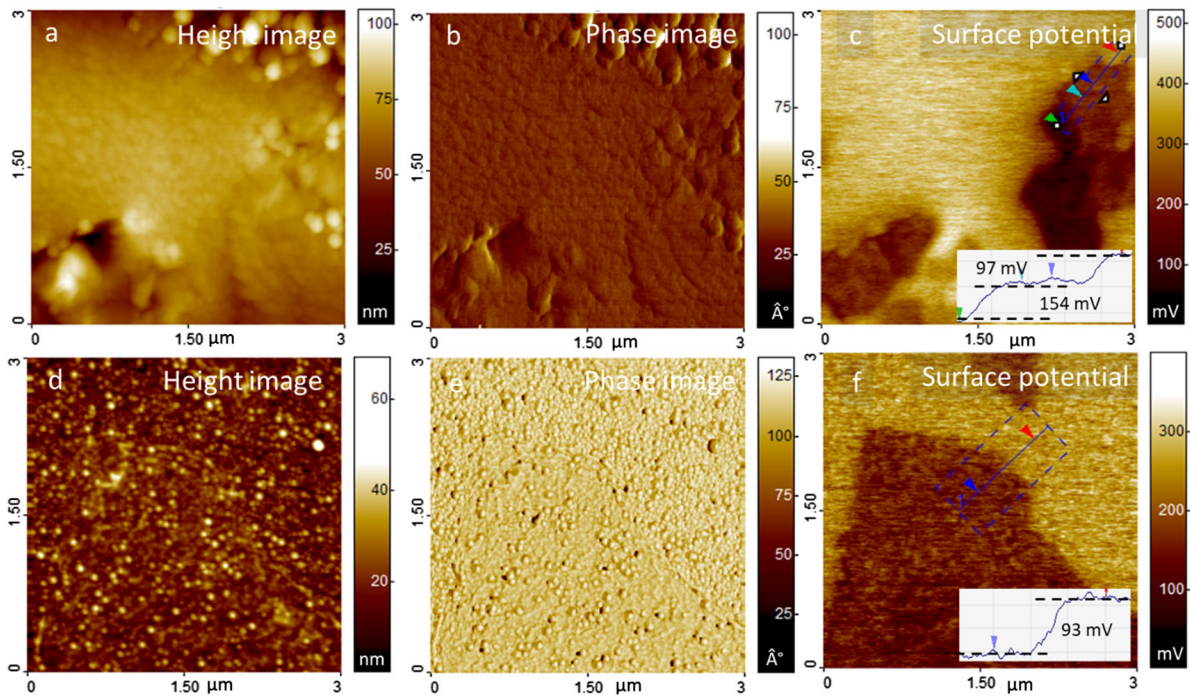


Fig. 1 AFM height and phase images, and also KPFM surface potential images of reduced graphene oxide on gold sputtered substrates: **a–c** rGO_C, **d–f** rGO_I

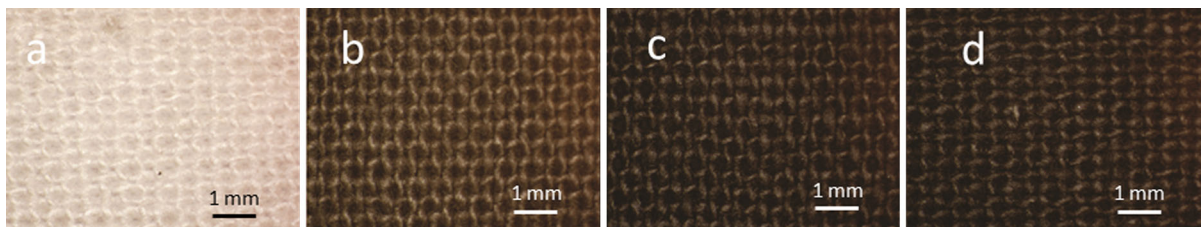


Fig. 2 Reflected light microscopy images of: **a** neat cotton fabric, **b** fGO, **c** fGO_C after GO reduction, **d** fGO_I after GO reduction

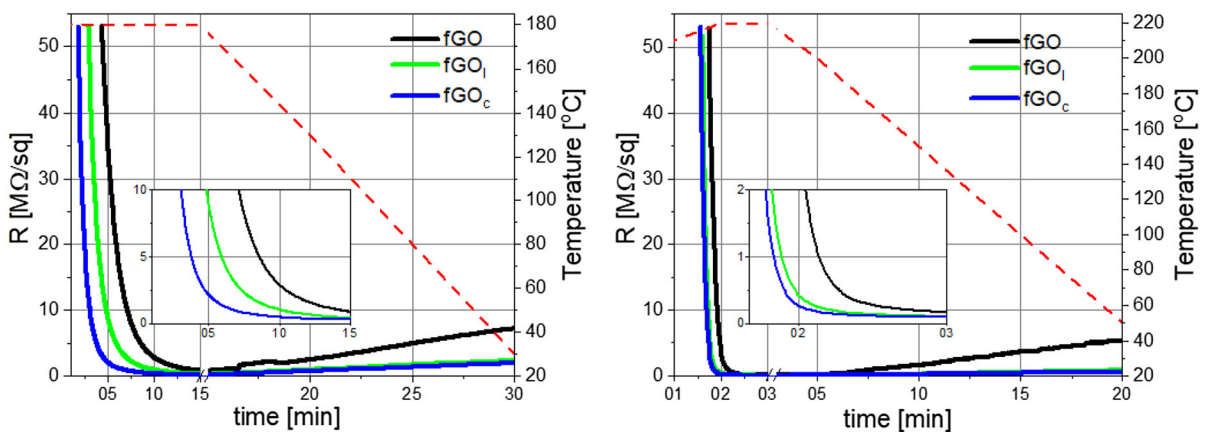


Fig. 3 Dependencies of surface resistivity, R , on time and temperature during annealing and subsequent cooling

of GO on the fiber surfaces. Figure 3 shows that at 180 °C R of the samples dropped below 50 M Ω /sq at the beginning of annealing, quickly decreased further with increasing annealing time and finally leveled off. During heating of the samples to 220 °C, the decrease of R to below 50 M Ω /sq began before the target temperature was reached, and the further decrease of R was much faster than at 180 °C; R leveled off within the first minute. Hence, the samples annealed at 180 °C were cooled to RT after 15 min, whereas those annealed at 220 °C after 1 min of annealing. In all cases, R increased during cooling and further increased at RT showing partial reversibility of the reduction. It is well known that at relatively low temperatures, below 250 °C, reduction of GO is incomplete (Acik et al. 2011; Huh 2011), and, according to our results, can be reverted to some extent during cooling and holding at RT in air. However, the increase of R of all the samples saturated at RT within 24 h. Others (Tegou et al. 2016) demonstrated that, contrary to heating in a vacuum or an inert atmosphere, heating in air triggered concomitant reduction and oxidation reactions. During thermal treatment of GO at the temperature up to 300 °C hydroxyl and epoxy groups were progressively eliminated, but at the same time, newly formed carbonyls appeared because of oxidation. Nevertheless, the amount of C=C bonds and the electrical conductivity increased. It must be noted that an increase of the reduction temperature of GO on cotton fabric would be beneficial for the reduction but at the same time it would be detrimental for the fabric.

The R values of the samples, reached after 15 min at 180 and after 1 min at 220 °C, R_{180} and R_{220} , respectively, together with those measured for the same samples after 24 h at RT, R_{180RT} and R_{220RT} , respectively, are plotted in Fig. 4 and listed in Table 1. In each case, the reduction at 220 °C yielded better results, reflected in the smaller R achieved in a shorter time. Both, vitamin C and Irganox 1010, accelerated the reduction and permitted to reach the lower R values at both temperatures. R of fGO_C decreased faster than that of fGO_I, especially at 180 °C, but the R_{180RT} and R_{220RT} of fGO_C exceeded those of fGO_I. Moreover, for fGO_I R_{180RT}/R_{220RT} ratio was 1.80, whereas the respective numbers for fGO and fGO_C were 5.2 and 2.7.

On SEM micrographs in Fig. 5 rGO platelets are practically unnoticeable, due to their small thickness

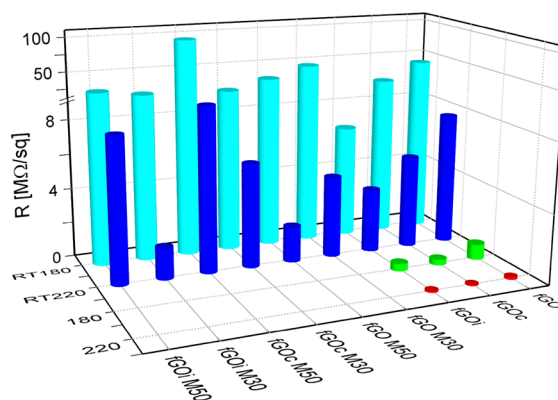


Fig. 4 The surface resistivity, R, of GO coated fabric samples, fGO, fGO_C, fGO_I; reached during reduction at 180 and 220 °C (180 and 220), attained at RT (180RT and 220RT), and also R values at RT (180RT and 220RT) of MTCS treated fabric specimens (fGO M30, fGO M50, fGO_C M30, fGO_C M50, fGO_I M30, fGO_I M50)

and tight adhesion to surfaces of the cotton fibers. In the same Fig. 5, static droplets on fabric sample surfaces after the reduction are shown. Prior to the reduction fGO and fGO_C were hydrophilic and water droplets soaked into them completely, whereas fGO_I was hydrophobic, with WCA of 132.9°. Surprisingly, after the reduction, the surface of fGO_C remained hydrophilic and the fabric absorbed water droplets, although after the reduction it was rinsed in water to remove water soluble products of the reactions, and next dried at RT. However, after deprotonation vitamin C converts to dehydroascorbic acid, and further to oxalic and gluconic acids, which might form hydrogen bonds with the residual oxygen-containing functional groups on the rGO surface (Zhang et al. 2010b). Another reason of hydrophilicity can be a change of GO platelet morphology during reduction with vitamin C. Others (De Silva et al. 2018) observed that the platelets fractured and became wavy. Indeed, after the reduction of GO in aqueous solution of vitamin C the platelets had smaller lateral sizes than after Irganox 1010 assisted reduction, as shown in Fig. 1. Possible fracture of the platelets can locally expose cellulose fibers and contribute to hydrophilicity of fGO_C after the reduction.

On the contrary, fGO and fGO_I after the reduction were hydrophobic, which is further corroborated by the WCA and WSA values listed in Table 1. It appears that the reduction at 220 °C led to the larger WCA and smaller WSA than the reduction at 180 °C. Moreover,

Table 1 The effect of GO reduction temperature, 180 and 220 °C, on water contact angles (WCA), sliding angles (WSA) and surface resistivity (R) of GO coated fabric samples; R_{180}

and R_{220} denote R reached at 180 and 220 °C, respectively, R_{180RT} and R_{220RT} denote R at RT

Sample code	180 °C				220 °C			
	R_{180} (M Ω /sq)	R_{180RT} (M Ω /sq)	WCA (°)	WSA (°)	R_{220} (M Ω /sq)	R_{220RT} (M Ω /sq)	WCA (°)	WSA (°)
fGO	0.90	40.0	138.1	20	0.17	7.7	147.5	10
fGO _C	0.32	14.8	–	–	0.10	5.4	–	–
fGO _I	0.43	6.6	140.4	15	0.11	3.7	142.4	8

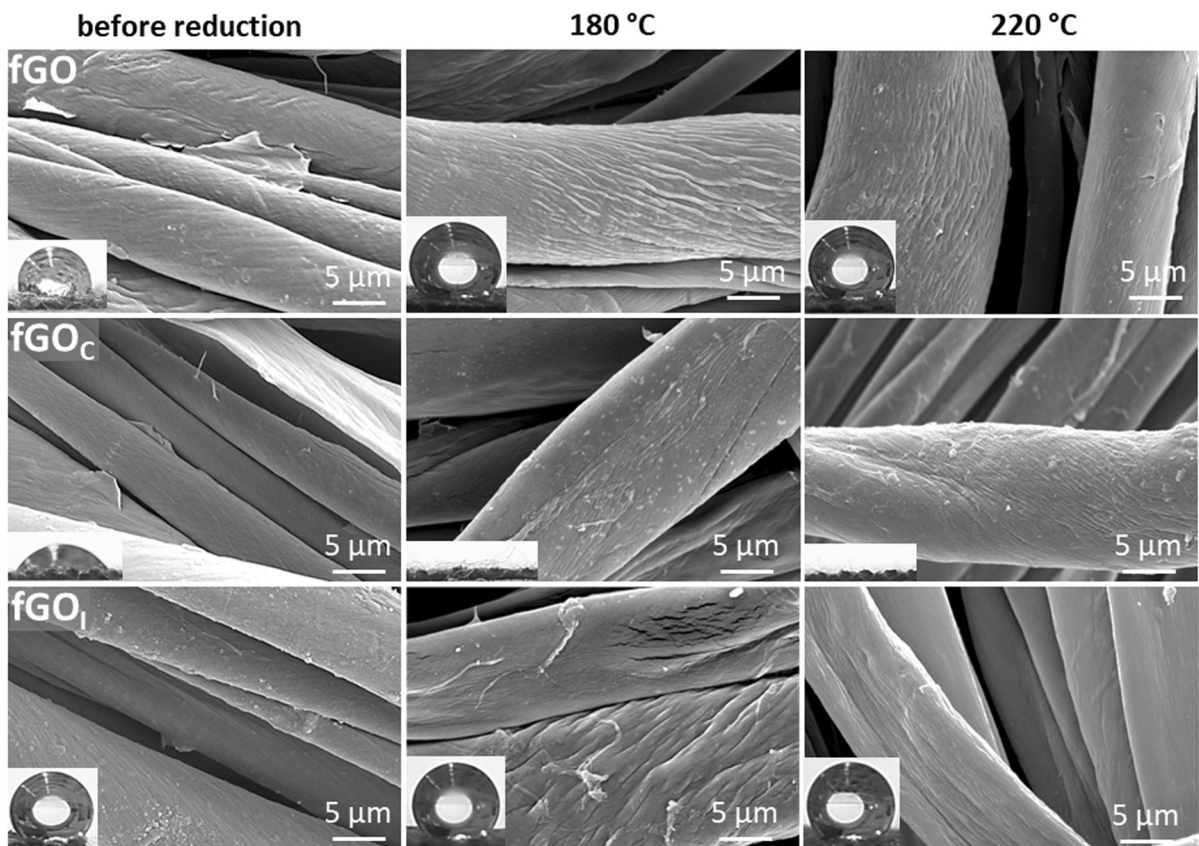


Fig. 5 SEM micrographs of fibers and photographs of static water droplets placed on surfaces of fGO, fGO_C (after 15 s) and fGO_I after reduction of GO at 180 and 220 °C

for both fGO and fGO_I the petal effect was observed, indicating an adhesive type of hydrophobicity as described by others (Tissera et al. 2015).

R_{180} , R_{220} , R_{180RT} and R_{220RT} values of the MTCS treated fabric samples are plotted in Fig. 4 and listed in Table 2, together with WSA and WCA values. MTCS treatment carried out after the reduction of GO permitted to achieve superhydrophobicity. The

smallest WCA values, about 165°–168°, were measured for fGO after reduction at 180 °C, whereas in all other cases the WCA values were close to or above 170°. This was accompanied by a decrease of WSA to 2°–3°. According to (Makowski et al. 2014) the MTCS treatment results in the formation of polymethylsilsesquioxane (PMSQ) micro- and nano-sized globular particles bonded to the modified surface through

Table 2 The effect of MTCS treatment on water contact angles (WCA), sliding angles (WSA) and a surface resistivity at RT (R_{180RT} and R_{220RT}) of MTCS treated fabric samples after GO reduction at 180 and 220 °C

Sample code	180 °C			220 °C		
	R_{180RT} (M Ω /sq)	WCA (°)	WSA (°)	R_{220RT} (M Ω /sq)	WCA (°)	WSA (°)
fGO M30	30.5	164.7	2	4.7	174.0	3
fGO M50	49.5	167.7	2	2.1	171.1	3
fGO _C M30	17.0	170.0	2	6.0	170.4	2
fGO _C M50	96.0	169.5	2	18.5	170.7	2
fGO _I M30	20.6	169.9	2	1.8	169.4	2
fGO _I M50	28.5	170.9	2	8.3	171.1	2

reaction of MTCS with hydroxyl groups. The presence of those particles was responsible for superhydrophobicity and the lotus effect. Indeed, SEM micrographs of MTCS modified fabric samples shown in Fig. 6 evidence the presence of PMSQ particles on the fiber surfaces. After conditioning at RH of 50%, more particles were formed, as seen on the SEM micrographs in Fig. 6, but the effect on WCA and WSA was rather minor, evidencing that the role of humidity level was not significant.

Obviously, the surface modification after the conditioning at RH of 30% was sufficient to achieve superhydrophobicity and a further increase of the number of PMSQ particles was not significant. It also appears that the lower temperature of GO reduction, 180 °C, prior to the conditioning at 30% RH, resulted in less uniform distribution of PMSQ particles on the surfaces, and in local clustering of the particles as exemplified in Fig. 7.

The effect of MTCS treatment on R of the fabric samples was different and depended on the sample tested, temperature of GO reduction, and RH during the conditioning. In general, R_{180RT} of all the materials increased, with the only exception of fGO M30. R_{220RT} decreased for fGO M30, fGO M50, and for fGO_I M30 compared to that of fGO and fGO_I. The changes in the R values might result from different phenomena, like reactions of MTCS with remaining rGO functional groups, water absorption and/or adsorption, and also from the adverse effect of the formed particles on the conductive network of rGO platelets. Nevertheless, for fGO M50 and fGO_I M30 the low R_{220RT} values of 2.1 and 1.8 M Ω /sq, respectively, were achieved. It is worth noting that although

R changed after the modification with MTCS, then it was stable in time.

Maximum force values measured during tensile testing of the fabric samples are collected in Table 3. It appears that after padding the fabric with GO dispersion and reduction of GO at 220 °C the maximum force diminished, especially for fGO_C. The MTCS treatment caused a further decrease of the force for fGO, and even more for fGO_C. Only for fGO_I the treatment did not have a negative effect, and the force remained practically the same within the limits of experimental error. It appears that Irganox limited the adverse effect of thermal and chemical treatment on the tensile strength of the GO coated cotton fabric.

Conclusions

Thermal reduction of GO in the presence pentaerythritol tetrakis(3-(3,5-di-*tert*-butyl-4-hydroxyphenyl)propionate)—Irganox 1010, an antioxidant widely used in the plastic industry, was carried out. The reduction of GO in an aqueous suspension containing this compound resulted in larger and better exfoliated rGO platelets than those obtained from the process carried out in the suspension with L-ascorbic acid—vitamin C, which was used for comparison.

The thermal reduction of GO deposited by the padding method on cotton fabric carried out in air at 180 or 220 °C, imparted electrical conductivity to the fabric, fGO, which was reflected in surface resistivity at RT, R, of 40 and 7.7 M Ω /sq, respectively. For GO coated fabric samples, fGO_C and fGO_I, which prior to the reduction were treated with vitamin C and with Irganox 1010, respectively, at RT even lower R values

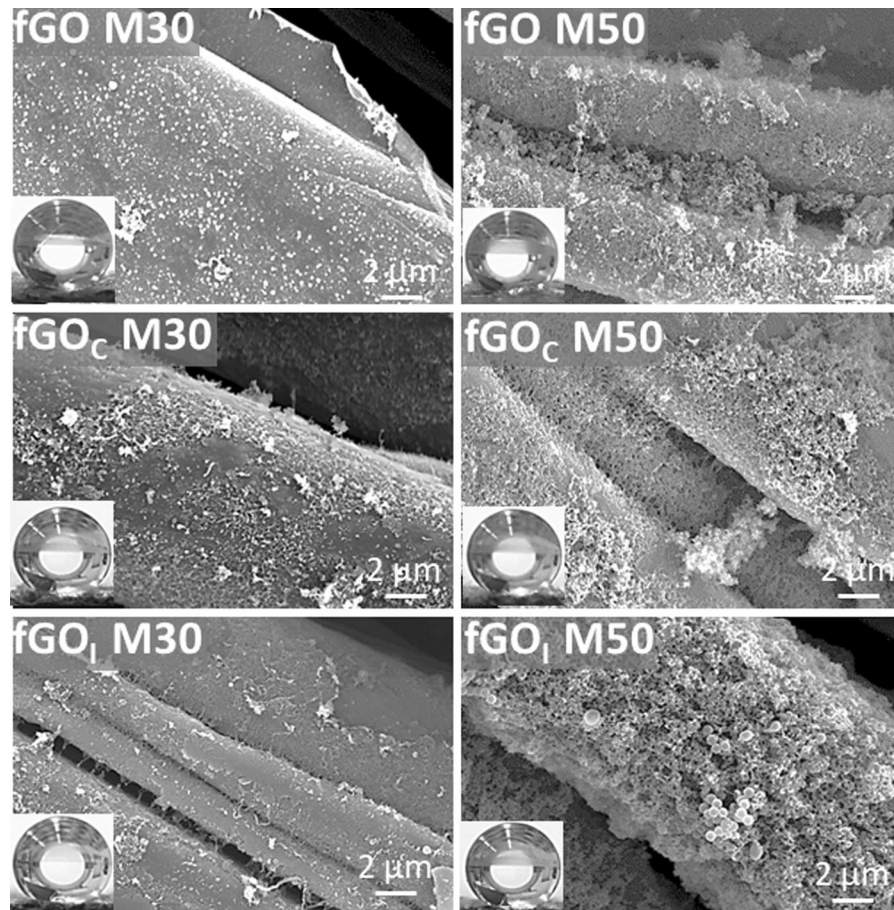


Fig. 6 SEM micrographs of fibers of fGO M50, fGO_C M50, fGO_I M50, conditioned at RH of 50%, and SEM micrographs of fibers and photographs of static water droplets on surfaces of

fGO M30, fGO_C M3, fGO_I M30, conditioned at RH of 30%, for which reduction of GO was carried out at 220 °C

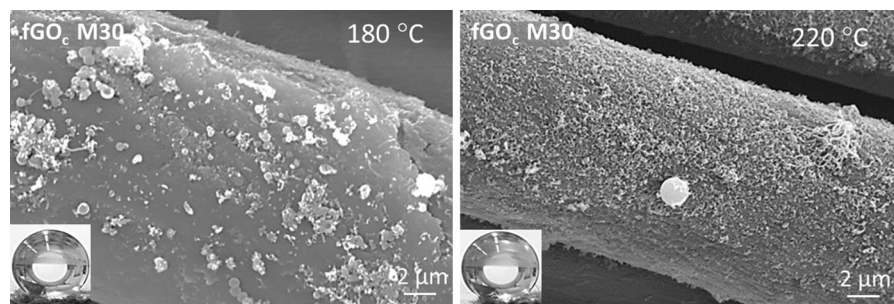


Fig. 7 The effects of temperature of GO reduction on modification of the surface of fGO_C M30

were reached. For all the materials R increased after the reduction during cooling and during the first hours of storage at RT. However, the most stable effect of GO reduction was achieved using Irganox 1010, which assisted the reduction of GO at both 180 and

220 °C, and allowed to obtain the cotton fabric with stable R values of 6.6 and 3.7 MΩ/sq, respectively. The modified cotton fabric can be used in applications where static electricity is a disadvantage or even a danger, for instance in protective cloth in explosive

Table 3 The effect of GO reduction at 220 °C and MTCS treatment (after conditioning at RH of 30%) on maximum force measured during tensile testing of fabric specimens

Sample code	Force (N)
Neat fabric	55.2
fGO	39.7
fGO _C	19.6
fGO _I	39.9
fGO M30	21.2
fGO _C M30	8.5
fGO _I M30	42.8

atmospheres. It can be also applied for electromagnetic radiation shielding.

fGO_I after the reduction was hydrophobic, unlike hydrophilic fGO_C. MTCS treatment resulting in the formation of PMSQ particles on the fiber surfaces permitted to impart superhydrophobicity and the lotus effect to the fabric. Although after MTCS treatment in most cases R increased, for fGO M50 and fGO_I M30 low values of 2.1 and 1.8 MΩ/sq, respectively, were obtained. Moreover, the use of Irganox 1010 limited the adverse effect of the thermal and chemical treatment on the tensile strength of the GO coated cotton fabric.

Acknowledgments The authors would like to thank for the financial support of this work from the National Science Centre Poland (UMO-2014/15/B/ST8/04286).

References

- Acik M, Lee G, Mattevi C, Pirkle A, Wallace RM, Chhowalla M, Cho K, Chabal Y (2011) The role of oxygen during thermal reduction of graphene oxide studied by infrared absorption spectroscopy. *J Phys Chem C* 115:19761–19781. <https://doi.org/10.1021/jp2052618>
- Attia NF, El Ebissy AA, Hassan MA (2015) Novel synthesis and characterization of conductive and flame retardant textile fabrics. *Polym Adv Technol* 26:1551–1557. <https://doi.org/10.1002/pat.3580>
- Bussy C, Jasim D, Lozano N, Terry D, Kostarelos K (2015) The current graphene safety landscape—a literature mining exercise. *Nanoscale* 7:6432–6435. <https://doi.org/10.1039/c5nr00236b>
- Chua CK, Pumera M (2014) Chemical reduction of graphene oxide: a synthetic chemistry viewpoint. *Chem Soc Rev* 43:291–312. <https://doi.org/10.1039/c3cs60303b>
- De Silva KKH, Huang H-H, Yoshimura M (2018) Progress of reduction of graphene oxide by ascorbic acid. *Appl Surf Sci* 447:338–346. <https://doi.org/10.1016/j.apsusc.2018.03.243>
- Fernandez-Merino MJ, Guardia L, Paredes JI, Villar-Rodil S, Solis-Fernandez P, Martinez-Alonso A, Tascon JMD

- (2010) Vitamin C Is an ideal substitute for hydrazine in the reduction of graphene oxide suspensions. *J Phys Chem C* 114:6426–6432. <https://doi.org/10.1021/jp100603h>
- Huang Y, Zhu MS, Pei ZX, Xue Q, Huang Y, Zhi CY (2016) A shape memory supercapacitor and its application in smart energy storage textiles. *J Mater Chem A* 4:1290–1297. <https://doi.org/10.1039/c5ta09473a>
- Huang Y, Gao L, Zhao YN, Guo XH, Liu CX, Liu P (2017) Highly flexible fabric strain sensor based on graphene nanoplatelet-polyaniline nanocomposites for human gesture recognition. *J Appl Polym Sci* 134:8. <https://doi.org/10.1002/app.45340>
- Huh SH (2011) Thermal reduction of graphene oxide. In: Mikhailov S (ed) *Physics and applications of graphene—experiments*. InTech, London, pp 73–90
- Jost K, Perez CR, McDonough JK, Presser V, Heon M, Dion G, Gogotsi Y (2011) Carbon coated textiles for flexible energy storage. *Energy Environ Sci* 4:5060–5067. <https://doi.org/10.1039/c1ee02421c>
- Juhász Z, Kitahara Y, Takahashi S, Fujii T (2012) Thermal stability of vitamin C: thermogravimetric analysis and use of total ion monitoring chromatograms. *J Pharm Biomed Anal* 59:190–193. <https://doi.org/10.1016/j.jpba.2011.10.011>
- Kiuru M, Alakoski E (2004) Low sliding angles in hydrophobic and oleophobic coatings prepared with plasma discharge method. *Mater Lett* 58:2213–2216. <https://doi.org/10.1016/j.matlet.2004.01.024>
- Makowski T, Kowalczyk D, Fortuniak W, Jeziorska D, Brzezinski S, Tracz A (2014) Superhydrophobic properties of cotton woven fabrics with conducting 3D networks of multiwall carbon nanotubes, MWCNTs. *Cellulose* 21:4659–4670. <https://doi.org/10.1007/s10570-014-0422-0>
- Marcato B, Guerra S, Vianello M, Scalia S (2003) Migration of antioxidant additives from various polyolefinic plastics into oleaginous vehicles. *Int J Pharm* 257:217–225. [https://doi.org/10.1016/S0378-5173\(03\)00143-1](https://doi.org/10.1016/S0378-5173(03)00143-1)
- Nooralian Z, Gashti MP, Ebrahimi I (2016) Fabrication of a multifunctional graphene/polyvinylphosphonic acid/cotton nanocomposite via facile spray layer-by-layer assembly. *RSC Adv* 6:23288–23299. <https://doi.org/10.1039/c6ra00296j>
- Onghena M, Van Hoeck E, Van Loco J, Ibanez M, Cherta L, Portoles T, Pitarch E, Hernandez F, Lemiere F, Covaci A (2015) Identification of substances migrating from plastic baby bottles using a combination of low-resolution and high-resolution mass spectrometric analysers coupled to gas and liquid chromatography. *J Mass Spectrom* 50:1234–1244. <https://doi.org/10.1002/jms.3644>
- Pei SF, Cheng HM (2012) The reduction of graphene oxide. *Carbon* 50:3210–3228. <https://doi.org/10.1016/j.carbon.2011.11.010>
- Pelin M, Fusco L, Leon V, Martin C, Criado A, Sosa S, Vazquez E, Tubaro A, Prato M (2017) Differential cytotoxic effects of graphene and graphene oxide on skin keratinocytes. *Sci Rep*. <https://doi.org/10.1038/srep40572>
- Poletto M, Pistor V, Zattera AJ (2013) Structural characteristics and thermal properties of native cellulose. In: Van De Ven TGM (ed) *Cellulose—fundamental aspects*. InTech, London, pp 45–68

- Rani M, Shim WJ, Han GM, Jang M, Song YK, Hong SH (2017) Benzotriazole-type ultraviolet stabilizers and antioxidants in plastic marine debris and their new products. *Sci Total Environ* 579:745–754. <https://doi.org/10.1016/j.scitotenv.2016.11.033>
- Ren JS, Wang CX, Zhang X, Carey T, Chen KL, Yin YJ, Torrisi F (2017) Environmentally-friendly conductive cotton fabric as flexible strain sensor based on hot press reduced graphene oxide. *Carbon* 111:622–630. <https://doi.org/10.1016/j.carbon.2016.10.045>
- Sahito IA, Sun KC, Arbab AA, Qadir MB, Jeong SH (2015) Graphene coated cotton fabric as textile structured counter electrode for DSSC. *Electrochim Acta* 173:164–171. <https://doi.org/10.1016/j.electacta.2015.05.035>
- Sahito IA, Sun KC, Arbab AA, Qadir MB, Choi YS, Jeong SH (2016) Flexible and conductive cotton fabric counter electrode coated with graphene nanosheets for high efficiency dye sensitized solar cell. *J Power Sources* 319:90–98. <https://doi.org/10.1016/j.jpowsour.2016.04.025>
- Shateri-Khalilabad M, Yazdanshenas ME (2013a) Fabricating electroconductive cotton textiles using graphene. *Carbohydr Polym* 96:190–195. <https://doi.org/10.1016/j.carbpol.2013.03.052>
- Shateri-Khalilabad M, Yazdanshenas ME (2013b) Preparation of superhydrophobic electroconductive graphene-coated cotton cellulose. *Cellulose* 20:963–972. <https://doi.org/10.1007/s10570-013-9873-y>
- Stalder AF, Kulik G, Sage D, Barbieri L, Hoffmann P (2006) A snake-based approach to accurate determination of both contact points and contact angles. *Colloids Surf A Physicochem Eng Asp* 286:92–103. <https://doi.org/10.1016/j.colsurfa.2006.03.008>
- Stalder AF, Melchior T, Muller M, Sage D, Blu T, Unser M (2010) Low-bond axisymmetric drop shape analysis for surface tension and contact angle measurements of sessile drops. *Colloids Surf A Physicochem Eng Asp* 364:72–81. <https://doi.org/10.1016/j.colsurfa.2010.04.040>
- Tegou E, Pseiropoulos G, Filippidou MK, Chatzandroulis S (2016) Low-temperature thermal reduction of graphene oxide films in ambient atmosphere: infra-red spectroscopic studies and gas sensing applications. *Microelectron Eng* 159:146–150. <https://doi.org/10.1016/j.mee.2016.03.030>
- Tissera ND, Wijesena RN, Perera JR, de Silva KMN, Amaratunge GAJ (2015) Hydrophobic cotton textile surfaces using an amphiphilic graphene oxide (GO) coating. *Appl Surf Sci* 324:455–463. <https://doi.org/10.1016/j.apsusc.2014.10.148>
- Xu P, Wei BQ, Cao ZY, Zheng J, Gong K, Li FX, Yu JY, Li QW, Lu WB, Byun JH, Kim BS, Yan YS, Chou TW (2015) stretchable wire-shaped asymmetric supercapacitors based on pristine and MnO₂ coated carbon nanotube fibers. *ACS Nano* 9:6088–6096. <https://doi.org/10.1021/acsnano.5b01244>
- Zhang J, Zhang F, Yang H, Huang X, Liu H, Zhang J, Guo S (2010a) Graphene oxide as a matrix for enzyme immobilization. *Langmuir* 26:6083–6085. <https://doi.org/10.1021/la904014z>
- Zhang JL, Yang HJ, Shen GX, Cheng P, Zhang JY, Guo SW (2010b) Reduction of graphene oxide via L-ascorbic acid. *Chem Commun* 46:1112–1114. <https://doi.org/10.1039/b917705a>
- Zhang XQ, Huang XX, Zhang XD, Zhong B, Xia L, Liu J, Pan H, Wen GW (2016) A facile method to prepare graphene-coat cotton and its application for lithium battery. *J Solid State Electrochem* 20:1251–1261. <https://doi.org/10.1007/s10008-016-3118-6>